

**Zeitschrift:** IABSE reports of the working commissions = Rapports des commissions de travail AIPC = IVBH Berichte der Arbeitskommissionen

**Band:** 13 (1973)

**Artikel:** Nonstationary hysteretic stress-strain relations of wide-flange steels and moment-curvature relations under presence of axial force

**Autor:** Yokoo, Yoshitsura / Nakamura, Tsuneyoshi / Komiyama, Toshiro

**DOI:** <https://doi.org/10.5169/seals-13760>

### **Nutzungsbedingungen**

Die ETH-Bibliothek ist die Anbieterin der digitalisierten Zeitschriften auf E-Periodica. Sie besitzt keine Urheberrechte an den Zeitschriften und ist nicht verantwortlich für deren Inhalte. Die Rechte liegen in der Regel bei den Herausgebern beziehungsweise den externen Rechteinhabern. Das Veröffentlichen von Bildern in Print- und Online-Publikationen sowie auf Social Media-Kanälen oder Webseiten ist nur mit vorheriger Genehmigung der Rechteinhaber erlaubt. [Mehr erfahren](#)

### **Conditions d'utilisation**

L'ETH Library est le fournisseur des revues numérisées. Elle ne détient aucun droit d'auteur sur les revues et n'est pas responsable de leur contenu. En règle générale, les droits sont détenus par les éditeurs ou les détenteurs de droits externes. La reproduction d'images dans des publications imprimées ou en ligne ainsi que sur des canaux de médias sociaux ou des sites web n'est autorisée qu'avec l'accord préalable des détenteurs des droits. [En savoir plus](#)

### **Terms of use**

The ETH Library is the provider of the digitised journals. It does not own any copyrights to the journals and is not responsible for their content. The rights usually lie with the publishers or the external rights holders. Publishing images in print and online publications, as well as on social media channels or websites, is only permitted with the prior consent of the rights holders. [Find out more](#)

**Download PDF:** 11.12.2025

**ETH-Bibliothek Zürich, E-Periodica, <https://www.e-periodica.ch>**

# **Nonstationary Hysteretic Stress-strain Relations of Wide-Flange Steels and Moment-Curvature Relations under Presence of Axial Force**

Relations hystérétiques non-stationnaires tension-déformation d'éléments en acier à ailes larges et relations moment-courbure en présence d'une force axiale

Nichtstationäre hysteretische Spannungs/Dehnungs-Beziehungen von Breitflanschstählen und Moment/Krümmungs-Beziehungen unter auftretender Axialkraft

**Yoshitsura YOKOO**  
Prof. Dr. Eng.

**Tsuneyoshi NAKAMURA**  
Assoc. Prof. Ph.D.Dr. Eng.  
Department of Architecture  
Kyoto University  
Kyoto, Japan

**Toshiro KOMIYAMA**  
M. Eng.

## **1. INTRODUCTION**

It is apparent from the review of the Introductory Report for Theme III that, while a number of experimental results have been presented on the load-deflection behaviors of steel members and frames subjected to repeated alternating loads, almost all the corresponding results of numerical analysis have been based upon either simplified bilinear hysteretic or extended Ramberg-Osgood relations without experimental verification. To the best of the authors' knowledge and as the Introductory Report for Theme I has pointed out particularly, experimental hysteretic stress-strain curves under alternating strain and stress cycling conditions have not been obtained systematically *for the purpose of deriving the stress-strain relations applicable to arbitrary nonstationary stress-strain paths*. Although some papers presenting experimental results on low-cycle fatigue of materials have included stress-strain curves obtained under mostly constant strain or stress amplitudes and discussed their shapes and energy absorption capacities, the principal aim seems to have been at the correlations between their stationary shapes and the low-cycle fatigue properties of various metals, not particularly of structural steel.

With this understanding of the state-of-the-art [1], the senior authors (Yokoo and Nakamura) have first presented in [2], a set of hysteretic and skeleton stress-strain relations for a wide-flange steel applicable to steady-state hysteresis loops of *completely reversed* strain cycling of constant strain amplitudes and then started a series of nonstationary tension-compression tests specifying stress-strain paths [4]. In this contribution to the prepared discussion, some of the recent test results and a set of nonlinear hysteretic stress-strain relations derived from the experimental stress-strain curves are first presented.

The senior authors have also presented the experimental load-deflection curves of beam-columns subjected to dead and alternating repeated loads [5] (obtained by forced deflection). For the purpose of predicting the nonstationary inelastic behavior of beam-columns subjected to combined axial and lateral forces, Nakamura

proposed in 1966 [6] a method of analysis based upon the sandwich idealization of the cross-sectional property of a wide-flange or box section. The principal aims of the sandwich formulation are, (1) the direct analytical derivation of the axial force-bending moment-curvature relation from bilinear or nonlinear hysteretic stress-strain relations, (2) the possibility of obtaining piecewise analytical solutions for flanges obeying bilinear hysteretic stress-strain relations, and (3) to develop a rational numerical method of analysis which incorporates nonlinear hysteretic stress-strain relations and the effect of large deflection, is able to trace gradual spreading and/or diminishing of strain-hardening regions but is so simple and compact that an available computer would be able to carry out numerical integration with respect to time even for plane frames of practical size. A numerical method for the aim (3) has been described in the senior authors' prepared discussion on Theme I. In the second part of this contribution, an experimental cyclic moment-curvature relation under a constant axial force is presented and compared with the analytical prediction due to the sandwich theory.

## 2. NONSTATIONARY TENSION-COMPRESSION TEST

**2.1 SPECIMEN** Fig.1 shows the shape and size of the specimens. A specimen was manufactured by shapering from a half-flange of a commercially available SS41 wide-flange steel of the nominal size 400×400×13×21. The chemical composition of the steel due to the millsheet is c 0.25%, Si 0.07%, Mn 0.62%, P 0.017% and S 0.013%.

**2.2 TEST SETUP** The senior authors devised a keyhole mechanism in [2] for gripping smaller plate specimens by modifying a commercially available gripping apparatus for cylindrical specimens. The gripping apparatus for the present plate specimens utilizes the same keyhole mechanism but is of a greater size and of a modified form suitable for an Autograph universal testing machine of capacity ±50 tons. Strain within the range of ±4% was measured by two pairs of precalibrated  $\Pi$ -gauges (shown in Fig.2) mounted on the four sides of a specimen symmetrically.

**2.3 CONTROL CONDITION** The tension-compression tests were carried out at the constant strain rate of 0.00044/sec., except the virgin paths in which the plastic flow plateaus appear. Table 1 shows the strain or stress paths prescribed for the present series of tests. A pair of amplitude limiters on the X-axis (strain axis) of the Autograph XY-recorder were moved manually in accordance with the prescribed strain cycling program.

**2.4 TEST RESULT** Fig.3 and 5 show two examples of experimental stress-strain curves under incompletely reversed strain cycling. Fig.4 shows a stress-strain curve in the tensile strain range, and Fig.6, in the compressive strain range.

## 3. NONSTATIONARY HYSTERETIC STRESS-STRAIN RELATIONS

In view of the purpose of incorporating stress-strain relations in finite element analysis of frames, it is considered appropriate to derive stress-strain relations in terms of the engineering strain  $\epsilon$  and the nominal stress  $\sigma$ . It is well-known that each smooth piece of hysteresis loops can be approximately represented by a (generalized) Ramberg-Osgood equation:

$$\frac{\epsilon - \epsilon_y^{(1)}}{\epsilon_y} = \frac{\sigma - \sigma_y^{(1)}}{\sigma_y} \left\{ 1 + \left( \frac{1}{a} \right)^r \left| \frac{\sigma - \sigma_y^{(1)}}{\sigma_y} \right|^{r-1} \right\}, \quad \begin{array}{l} \sigma_y: \text{the yield stress,} \\ \epsilon_y: \text{the yield strain.} \end{array} \quad (1)$$

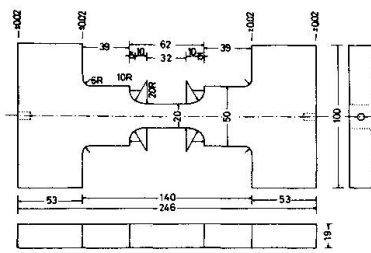


Fig. 1

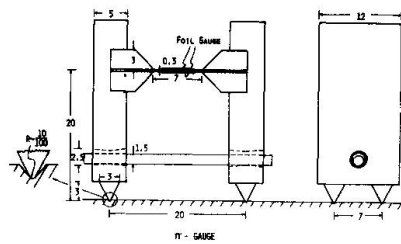


Fig. 2

Table 1 Specification of controlled strain paths and stress paths

| Specimen   | No.    | Reversal point-numbers and strains (%) or stresses |                 |      |                 |      |                 |      |                 |      |                 |      |      |      |      |      |                                  |
|--|--------|--|-----------------|------|-----------------|------|-----------------|------|-----------------|------|-----------------|------|------|------|------|------|----------------------------------|
|  |        | 1  | 2               | 3    | 4               | 5    | 6               | 7    | 8               | 9    | 10              | 11   | 12   | 13   | 14   | 15   |                                  |
| Incomplete alternating strain cycling $\epsilon(1) \geq 0$ | SS-14Z | -1.0   | +0.5            | -1.5 | +1.0            | -2.0 | +1.5            | -0.5 | +2.0            | -1.0 | +0.5            | -2.0 |      |      |      |      | Reversal point-strain controlled |
|  | SS-7Z  | -1.0   | +1.5            | -1.5 | +2.0            | -2.0 | +0.5            | -0.5 | +1.0            | -1.0 | +1.5            | -2.0 |      |      |      |      |                                  |
|  | SS-13Z | -1.5   | +1.0            | -2.0 | +1.5            | -0.5 | +2.0            | -1.0 | +0.5            | -1.5 | +1.0            | -2.5 | +2.5 | -3.0 | +3.0 | -3.0 |                                  |
|  | SS-12Z | -1.5   | +2.0            | -2.0 | +0.5            | -0.5 | +1.0            | -1.0 | +1.5            | -1.5 | +2.0            | -2.5 | +2.5 | -3.0 | +3.0 |      |                                  |
|  | SS-10S | -2.0   | +2.0            | -3.0 | +3.0            | -4.0 | +4.0            | -1.0 | +1.0            | -2.0 | +2.0            | -4.0 |      |      |      |      |                                  |
|  | SS-9S  | -2.0   | +4.0            | -3.0 | +1.0            | -4.0 | +2.0            | -1.0 | +3.0            |      |                 |      |      |      |      |      |                                  |
|  | SS-15S | -3.0   | +1.0            | -1.0 | +2.0            | -2.0 | +3.0            | -3.0 | +1.0            | -1.0 | +2.0            | -4.0 | +4.0 | -4.0 |      |      |                                  |
|  | SS-16S | -3.0   | +3.0            | -1.0 | +1.0            | -2.0 | +2.0            | -3.0 | +3.0            | -1.0 | +1.0            | -4.0 |      |      |      |      |                                  |
| One-way strain cycling $\epsilon(1) < 0$                   | SS-11S | -1.5   | 0               | -2.0 | 0               | -0.5 | 0               | -1.0 | 0               | -1.5 | 0               | -2.0 | 0    |      |      |      | Reversal point-stress controlled |
|  | SS-5S  | -3.0   | 0               | -4.0 | 0               | -1.0 | 0               | -2.0 | 0               | -3.0 | 0               | -4.0 | 0    |      |      |      |                                  |
|  | SS-3Z  | +1.5   | 0               | +2.0 | 0               | +0.5 | 0               | +1.0 | 0               | +1.5 | 0               | +2.0 | 0    |      |      |      |                                  |
|  | SS-2Z  | +3.0   | 0               | +4.0 | 0               | +1.0 | 0               | +2.0 | 0               | +3.0 | 0               | +4.0 | 0    |      |      |      |                                  |
|  | SS-4S  |  | +0.2 $\sigma_y$ |      | +0.4 $\sigma_y$ |      | +0.6 $\sigma_y$ |      | +0.8 $\sigma_y$ |      | +1.0 $\sigma_y$ |      |      |      |      |      |                                  |
|  | SS-6Z  |  | -0.2 $\sigma_y$ |      | -0.4 $\sigma_y$ |      | -0.6 $\sigma_y$ |      | -0.8 $\sigma_y$ |      | -1.0 $\sigma_y$ |      |      |      |      |      |                                  |
|  |        |  |                 |      |                 |      |                 |      |                 |      |                 |      |      |      |      |      |                                  |
|  |        |  |                 |      |                 |      |                 |      |                 |      |                 |      |      |      |      |      |                                  |

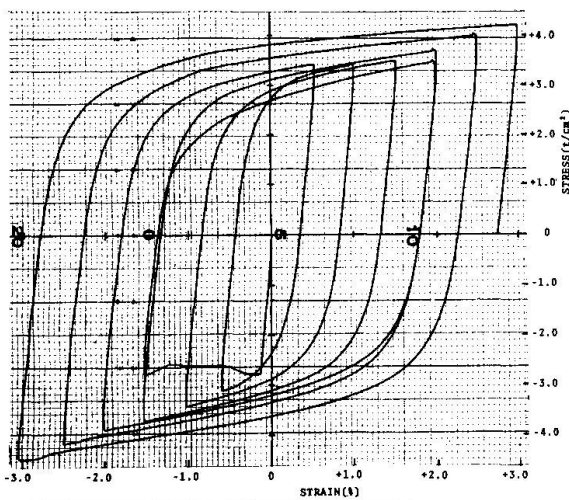


Fig. 3.

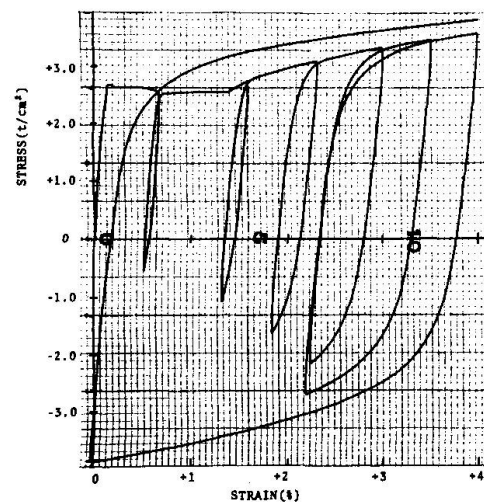


Fig. 4

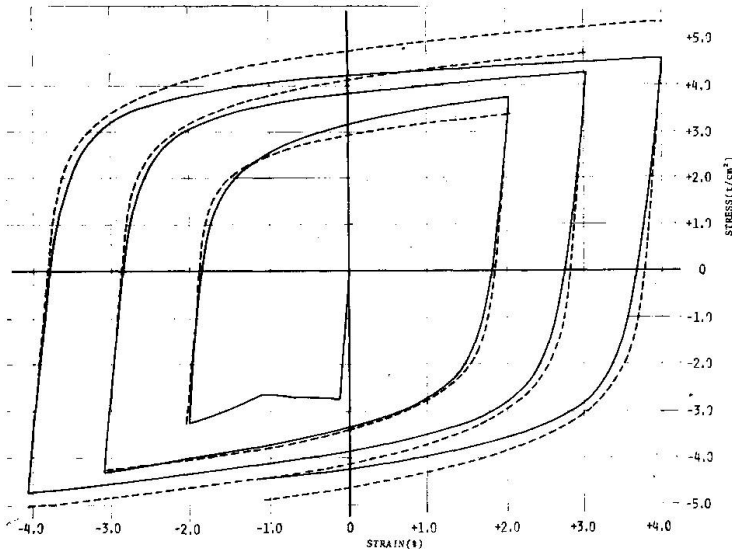


Fig. 5. COMPARISON OF EXPERIMENTAL AND APPROXIMATE STRESS-STRAIN CURVES

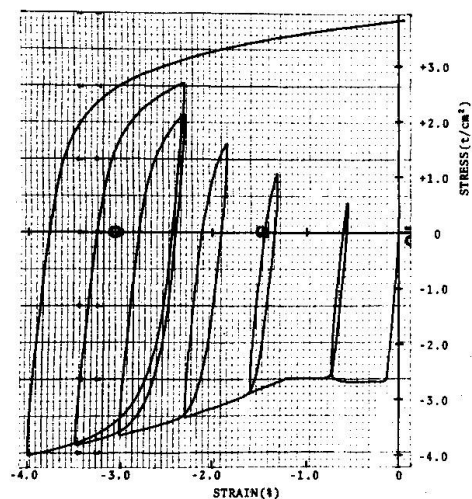


Fig. 6

where  $\epsilon^{(i)}$  and  $\sigma^{(i)}$  denote the  $i$ -th reversal point strain and stress, respectively and where  $a$  and  $r$  are the parameters which may depend upon various factors discussed below. Based upon the test results on the smaller plate specimens, the authors have presented a preliminary investigation [4] concerning the dependence of  $a$  and  $r$  not only upon  $\epsilon^{(i)}$  and  $\sigma^{(i)}$  but also upon other factors related to previous strain histories.

**3.1 RETURN BEHAVIOR** It should first be noticed that the steel has exhibited a return behavior on such a stress-strain curve as illustrated by Fig.4 or 6. It is apparently necessary to propose separate approximating equations for the virgin curve and for such loops as  $R_1R_2$  and  $R_2R_3$  indicated in Fig.7.

**3.2 FACTORS AFFECTING  $r$**  The usual log-log plot of the plastic strain component  $\epsilon - \epsilon^{(i)}$  and stress  $\sigma - \sigma^{(i)}$  for a smooth piece of a hysteresis loop would exhibit more deviation from a straight line (determined by the least square method) as the plot include those points within the range  $|\epsilon - \epsilon^{(i)}| \leq 2\epsilon_y$ . While it may be necessary to determine  $r$  for several different current strain ranges piecewisely if a higher accuracy of fitting is desirable, the averages for  $|\epsilon^{tip} - \epsilon^{(i)}| \geq 2\epsilon_y$  without regard to the current strain ranges have been determined for the six different groups of curves mentioned in 3.3 for the convenience of their applications.

**3.3 FACTORS AFFECTING  $a$**  Among various factors affecting  $a$ , it has been found in [4] and in this series that the most significant factor is apparently  $\sigma^{(i)}/\sigma_y$ . Fig.8 shows the plot of  $a$  with respect to  $\sigma^{(i)}/\sigma_y$ . Fig.9 shows the same plot for the previous smaller plate specimens.

**3.4 NONSTATIONARY HYSTERETIC STRESS-STRAIN RELATIONS** The following six sets of  $a$  and  $r$  have been derived from the test result.

(A1) Compressive path:  $\dot{\epsilon} < 0$  and  $1.1 < \sigma^{(i)}/\sigma_y < 1.7$ ,  
 $a = 1.421(\sigma^{(i)}/\sigma_y) + 0.026$ ,  $r = 8.89$ . (2.1)

(A2) Compressive path returning to the virgin curve:  
 $a = 0.609(\sigma^{(i)}/\sigma_y) + 1.358$ ,  $r = 7.80$  (2.2) for  $\epsilon^{(i)} < 0$ ,  $0.6 < \sigma^{(i)}/\sigma_y < 1.1$ .

(A3) Virgin compression path:  
 $a = 0.483$ ,  $r = 2.97$ . (2.3)

(B1) Tensile path:  $\dot{\epsilon} > 0$  and  $-1.9 < \sigma^{(i)}/\sigma_y < -1.0$ ,  
 $a = -1.350(\sigma^{(i)}/\sigma_y) + 0.222$ ,  $r = 10.95$ . (2.4)

(B2) Tensile path returning to the virgin curve:  
 $a = -0.505(\sigma^{(i)}/\sigma_y) + 1.325$ ,  $r = 7.96$  (2.5) for  $\epsilon^{(i)} > 0$ ,  $-1.1 < \sigma^{(i)}/\sigma_y < -0.6$ .

(B3) Virgin tensile path:  
 $a = 0.506$ ,  $r = 3.40$ . (2.6)

In drawing an approximating curve in accordance with one of the above formulae, it has been found that the curve is very sensitive to the value of  $a$ . While the above six sets of  $a$  and  $r$  are considered to be the minimum number of formulae, a slight improvement in  $a[\sigma^{(i)}/\sigma_y]$  can be attained by classifying the paths of (A1) and (B1) in accordance with Table 1 as follows:

For incompletely reversed strain cycling path;

(A11)  $a = 1.212(\sigma^{(i)}/\sigma_y) + 0.328$ ,  $r = 9.09$  ( $\dot{\epsilon} < 0$ ) (2.7)

(B11)  $a = -1.464(\sigma^{(i)}/\sigma_y) + 0.039$ ,  $r = 11.04$  ( $\dot{\epsilon} > 0$ ) (2.8)

For one-way strain cycling path;

(A12)  $a = 1.894(\sigma^{(i)}/\sigma_y) - 0.579$ ,  $r = 8.52$  ( $\dot{\epsilon} < 0$ ) (2.9)

(B12)  $a = -1.083(\sigma^{(i)}/\sigma_y) + 0.618$ ,  $r = 10.55$  ( $\dot{\epsilon} > 0$ ) (2.10)

Fig. 5 shows the approximating curve based upon (2.7) and (2.8).

Fig.10 shows the curve drawn with (2.2), (2.3) and (2.10).

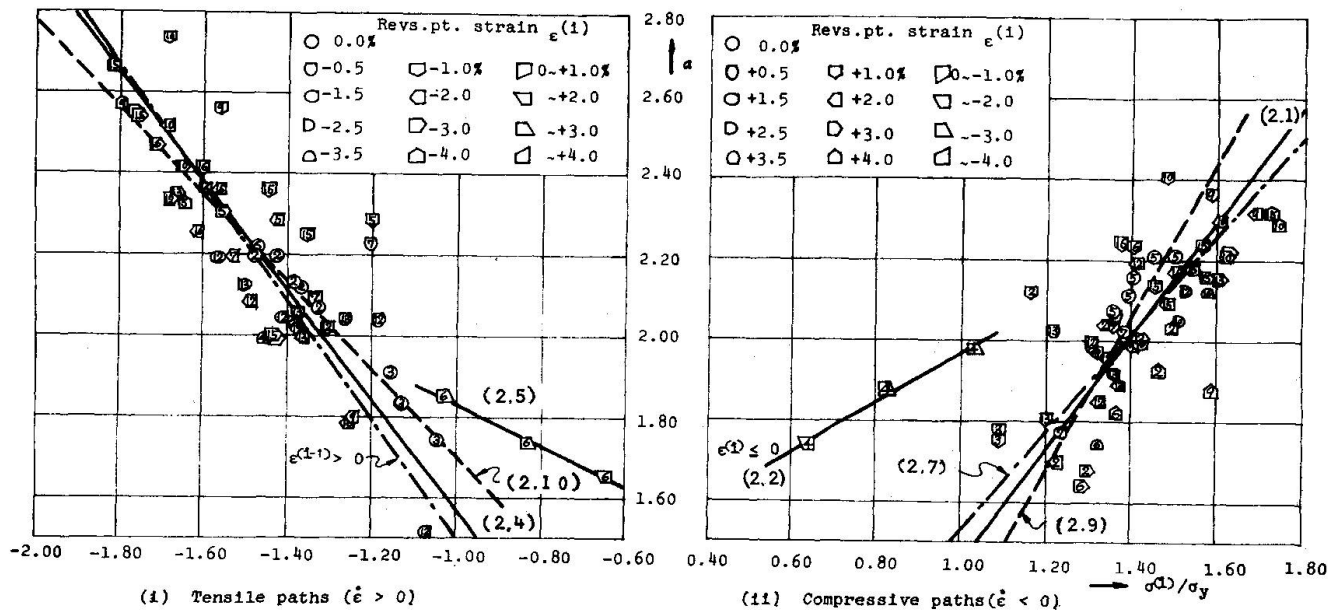


Fig. 8

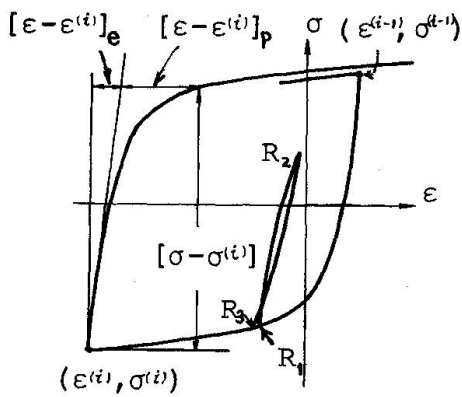


Fig. 7

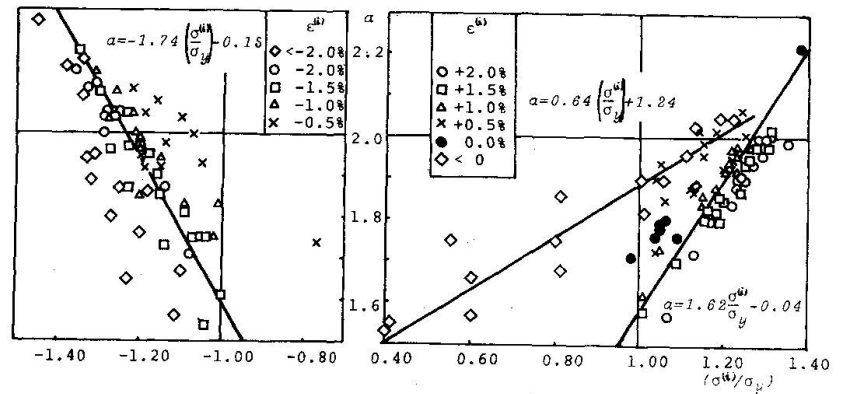


FIG. 9

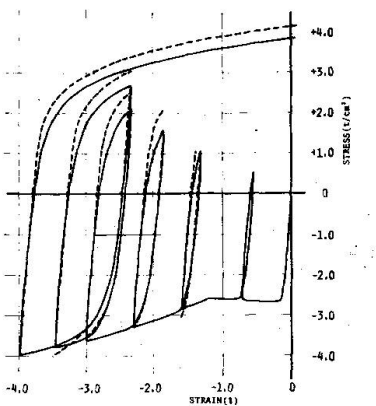


Fig. 10. COMPARISON OF EXPERIMENTAL AND APPROXIMATE STRESS-STRAIN CURVES

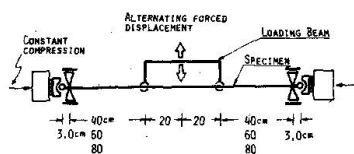
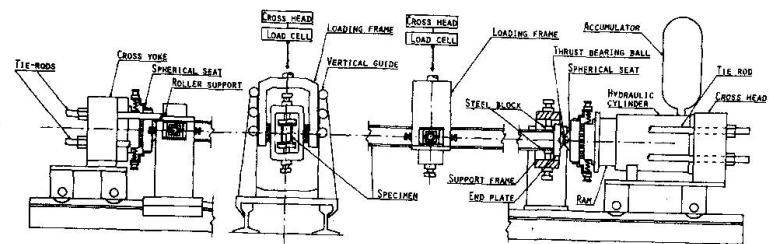


Fig. 11 SCHEMATIC DIAGRAM OF TEST CONDITIONS



SCHEMATIC DIAGRAM OF THE LOADING APPARATUS

Fig. 13.

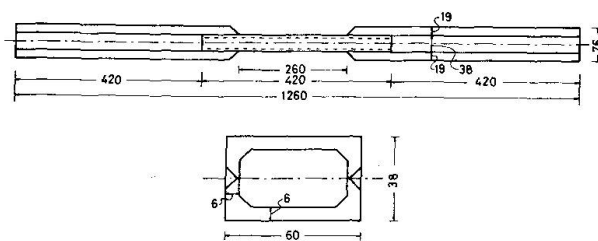


Fig. 12.

TEST SPECIMEN FOR  $M(N)-\epsilon$  RELATIONS



#### 4. ALTERNATING PLASTIC BENDING TEST UNDER AXIAL FORCE

Fig.11 shows the schematic diagram of the test and Fig.12 the test specimen. Fig.13 shows the schematic diagram of the loading apparatus. An example of the nondimensionalized experimental moment-curvature curve under a constant axial force ratio of -0.505 is shown in Fig.14.

#### 5. SANDWICH THEORY

The cross-sectional properties of an actual wide-flange section can be approximated by the idealized sandwich section whose two thin flanges have the half area, respectively and are located at the radius of gyration [6.7]. The nondimensionalized moment-curvature relation for the idealized sandwich section may directly be derived from Eq.(1) as follows.

$$\kappa - \kappa^{(i)} = (m - m^{(i)}) \left\{ 1 + \frac{1}{2} \left( \frac{1}{a_c} \right)^{r_c} |m - m^{(i)}|^{r_c - 1} + \frac{1}{2} \left( \frac{1}{a_r} \right)^{r_r} |m - m^{(i)}|^{r_r - 1} \right\} \quad (3)$$

where  $(a_c, r_c)$  and  $(a_r, r_r)$  denote  $(a, r)$  for  $\dot{\epsilon} < 0$  and  $\dot{\epsilon} > 0$ , respectively. A slight modification must be made for those portions after the returning points mentioned above and for initial portions corresponding to the plastic flow plateaus. The moment-curvature curve predicted by the theory is shown in Fig.14 by a dashed line and may be seen to fit the experimental curve fairly well at least during the first two cycles.

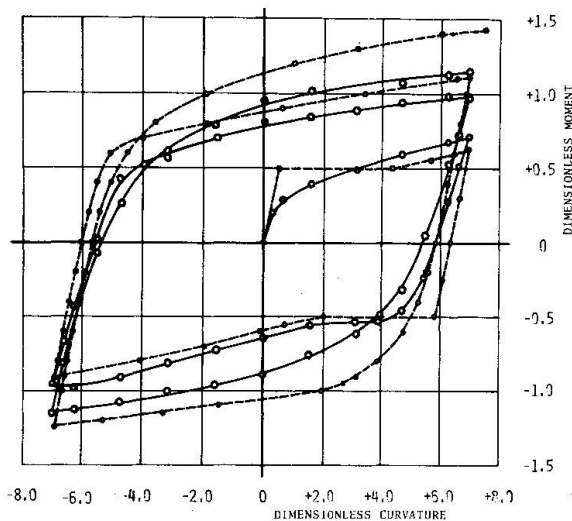


Fig.14 NON-DIMENSIONALIZED MOMENT-CURVATURE RELATION

#### References

- [1] Ryo Tanabashi, Yoshitsura Yokoo, Minoru Wakabayashi, Tsuneyoshi Nakamura, Haruo Kunieda, Hiroyuki Matsunaga and Toshihiko Kubota, "Load-deflection Behaviors and Plastic Fatigue of Wide-flange Beams Subjected to Alternative Plastic Bending, I Experimental Investigation", Trans. A.I.J. No. 175 (Sept. 1970) pp. 17-29.
- [2] Ryo Tanabashi, Yoshitsura Yokoo, Tsuneyoshi Nakamura, Toshihiko Kubota and Asao Yamamoto, "Load-deflection Behaviors and Plastic Fatigue of Wide-flange Beams Subjected to Alternating Plastic Bending, II Hysteretic and Skeleton Stress-strain Relations and Plastic Fatigues", Trans. A.I.J. No. 176 (Oct. 1970), pp. 25-36.
- [3] Ryo Tanabashi, Yoshitsura Yokoo and Tsuneyoshi Nakamura, "Load-deflection Behaviors and Plastic Fatigue of Wide-flange Beams Subjected to Alternating Plastic Bending, III Steady-state Theory", Trans. A.I.J. No. 177 (Nov. 1970), pp. 35-46.
- [4] Yoshitsura Yokoo, Tsuneyoshi Nakamura, Keishi Isoda and Toshiro Komiyama, "Nonstationary Hysteretic Stress-strain Relations of Wide-flange Steel," Summaries of Technical Papers presented at Annual Meeting (Kyushu) of Architectural Institute of Japan 1972, pp1299-1300.
- [5] Ryo Tanabashi, Yoshitsura Yokoo, Minoru Wakabayashi, Tsuneyoshi Nakamura and Haruo Kunieda, "Deformation History Dependent Inelastic Stability of Columns Subjected to Combined Alternating Loading", Proc. 1971 RILEM International Symposium on Experimental Analysis of Instability Problems on Reduced and Full-scale Models, Buenos Aires, Sept. 1971, Vol. III, pp. 275-295.
- [6] Tsuneyoshi Nakamura, "Elastic-plastic Behavior of a Linear Strain-hardening Sandwich Column Subjected to Alternating Lateral Force," Summaries of Tech. Papers presented at Annual Meeting of Archit. Inst. Japan, p285.
- [7] Tsuneyoshi Nakamura, "Methods of Elastic-plastic Analysis of Structures," (Dissertation for Dr.Eng., Kyoto University), Chap.6, Dec. 1970.

#### SUMMARY

Nonstationary hysteretic stress-strain curves have been presented from our recent systematic experimental investigation. A set of constitutive equations have been derived from the result. An experimental moment-curvature curve under a constant axial force has been presented and shown to be predicted by a sandwich theory based upon the constitutive equations with a considerably good accuracy.

## RESUME

Nous avons présenté une courbe hystérétique non-stationnaire tension-déformation qui a été dérivée de nos récentes recherches expérimentales systématiques. Une série d'équations constitutives a été dérivée du résultat. Nous avons présenté un diagramme moment-courbure sous une force axiale constante, et démontré qu'une théorie "sandwich" basée sur les équations constitutives conduisait au même résultat avec une précision considérable.

## ZUSAMMENFASSUNG

Die Arbeit zeigt nicht-stationäre hysteretische Spannungs-Dehnungs-Kurven unserer kürzlichen systematischen Untersuchungen. Eine Gruppe von Grundgleichungen wurde aus dem Resultat abgeleitet. Es wird eine experimentelle Momenten-Krümmungs-Kurve unter einer konstanten Axialkraft gezeigt und ihre gute Uebereinstimmung mit den nach der Sandwich-Theorie (basiert auf den Grundgleichungen) vorausgesagten Werten dargelegt.



Leere Seite  
Blank page  
Page vide